8-1-2009

Functional complementation of the Arabidopsis thaliana psbo1 mutant phenotype with an N-terminally His_6-tagged PsbO-1 protein in photosystem II

Haijun Liu
Louisiana State University

Laurie K. Frankel
Louisiana State University

Terry M. Bricker
Louisiana State University

Recommended Citation

Liu, H., Frankel, L., & Bricker, T. (2009). Functional complementation of the Arabidopsis thaliana psbo1 mutant phenotype with an N-terminally His_6-tagged PsbO-1 protein in photosystem II. *Biochimica et Biophysica Acta - Bioenergetics, 1787* (8), 1029-1038. https://doi.org/10.1016/j.bbabio.2009.03.006

Biochimica et Biophysica Acta 1787 (2009) 1029–1038

Contents lists available at ScienceDirect

Biochimica et Biophysica Acta

journal homepage: www.elsevier.com/locate/bbabio

Functional complementation of the *Arabidopsis thaliana psbo1* mutant phenotype with an N-terminally His_6-tagged PsbO-1 protein in photosystem II

Haijun Liu, Laurie K. Frankel, Terry M. Bricker *

Department of Biological Sciences, Division of Biochemistry and Molecular Biology, Louisiana State University, Baton Rouge, LA 70803, USA

ARTICLE INFO

Article history:
Received 16 January 2009
Received in revised form 3 March 2009
Accepted 6 March 2009
Available online 13 March 2009

Keywords:
Photosystem II
PsbO
Manganese-stabilizing protein
33 kDa protein
psbo1 mutant
Arabidopsis thaliana

ABSTRACT

The *Arabidopsis thaliana* mutant *psbo1* has recently been described and characterized. Loss of expression of the PsbO-1 protein leads to a variety of functional perturbations including elevated levels of the PsbO-2 protein and defects on both the oxidizing- and reducing-sides of Photosystem II. In this communication, two plant lines were produced using the *psbo1* mutant as transgenic host, which contained an N-terminally histidine$_6$-tagged PsbO-1 protein. This protein was expressed and correctly targeted into the thylakoid lumen. Immunological analysis indicated that different levels of expression of the modified PsbO-1 protein were obtained in different transgenic plant lines and that the level of expression in each line was stable over several generations. Examination of the Photosystem II closure kinetics demonstrated that the defective double reduction of Q_B and the delayed exchange of Q_BH_2 with the plastoquinone pool which were observed during the characterization of the *psbo1* mutant were effectively restored to wild-type levels by the His_6-tagged PsbO-1 protein. Flash fluorescence induction and decay were also examined. Our results indicated that high expression of the modified PsbO-1 was required to increase the ratio of PS II_α/PS II_β reaction centers to wild-type levels. Fluorescence decay kinetics in the absence of DCMU indicated that the expression of the His_6-tagged PsbO-1 protein restored efficient electron transfer to Q_B, while in the presence of DCMU, charge recombination between Q_A^- and the S_2 state of the oxygen-evolving complex occurred at near wild-type rates. Our results indicate that high expression of the His_6-tagged PsbO-1 protein efficiently complements nearly all of the photochemical defects observed in the *psbo1* mutant. Additionally, this study establishes a platform on which the in vivo consequences of site-directed mutagenesis of the PsbO-1 protein can be examined.

1. Introduction

Photosystem II (PS II) functions as a light-driven, water-plastoquinone oxidoreductase in higher plants and cyanobacteria. At least six intrinsic proteins appear to be required for O_2 evolution [1]. These are CP47, CP43, D1, D2, and the α and β subunits of cytochrome b_{559}. Additionally, in higher plants, three extrinsic proteins, with apparent molecular masses of 33 (PsbO), 24 (PsbP), and 16 kDa (PsbQ), are required for maximal rates of O_2 evolution at physiological inorganic cofactor concentrations [2,3]. Of these three proteins, the PsbO protein appears to play a central role in the stabilization of the manganese cluster and is essential for efficient and stable O_2 evolution [4]. Additionally, in higher plants, this component is required for PS II assembly/stability, and in the absence of the PsbO protein *Arabidopsis thaliana* cannot grow photoautotrophically [5].

In *A. thaliana*, two genes that encode PsbO (*psbO-1*, At5g66570, and *psbO-2*, At3g50820) are expressed under normal growth conditions, yielding two different PsbO proteins (PsbO-1 and PsbO-2, respectively). The PsbO-1 protein was reported to be nine times more abundant than the PsbO-2 protein [6]. It is unclear what advantage the plant would accrue from expressing two isoforms of the PsbO protein. Recently it has been reported that the PsbO-2 protein in *A. thaliana* can specifically regulate dephosphorylation and turnover of the PSII reaction center D1 protein [7]. Additionally, under long-term, low temperature growth conditions, the PsbO-1 protein is down-regulated and the PsbO-2 protein is up-regulated [8].

A high fluorescence mutant, *psbo1*, was recently identified in which a stop codon had been introduced into the *psbO-1* gene by EMS mutagenesis at amino acid residue 74 of the mature PsbO protein (^{74}Gln Stop), which led to the loss of this component [9]. The mutant exhibited a lower F_V/F_M, lower rates of steady state O_2 evolution, and

Abbreviations: CaMV, Cauliflower Mosaic Virus; DCMU, 3-(3,4-dichlorophenyl)-1,1-dimethylurea; EMS, ethane methyl sulfonate; LiDS, lithium dodecyl sulfate, MES, 2-[N-morpholino]ethanesulfonic acid; MS medium, Murashige and Skoog medium; PS I, Photosystem I; PS II, Photosystem II; PAGE, polyacrylamide gel electrophoresis; PVDF, polyvinylidene fluoride; Tricine, *N*-[2-hydroxy-1,1- bis(hydroxymethyl) ethyl]glycine

* Corresponding author. Tel.: +1 225 578 1555; fax: +1 225 578 2597.
E-mail address: btbric@lsu.edu (T.M. Bricker).

0005-2728/$ – see front matter © 2009 Elsevier B.V. All rights reserved.
doi:10.1016/j.bbabio.2009.03.006

retarded growth. It was demonstrated that the PsbO-1 protein is the major isoform in wild type under normal growth conditions and that in the *psbo1* mutant the PsbO-2 protein is up-regulated in a semi-compensatory manner. The mechanism that leads to the increased accumulation of the PsbO-2 protein in the *psbo1* thylakoid lumen is unclear at this time. These authors concluded that in mature leaves the total amount of the PsbO proteins in the *psbo1* mutant is somewhat lower than in wild type, although this difference is small. Domain-swapping analysis [6] followed by in vitro reconstitution experiments were interpreted as indicating that three amino acid differences between the PsbO-1 and PsbO-2 components (^{186}V to ^{186}S, ^{204}V to ^{204}I, and ^{246}L to ^{246}I) could explain the functional differences between the two PsbO proteins with respect to oxygen evolution. These authors concluded that both the lower expression level of the PsbO-2 protein and inherent functional defects of this component are responsible for the phenotype observed in the mutant *psbo1*.

Although data from these studies demonstrated that lower O_2 evolution activity occurred upon the binding of PsbO-2 in vivo [9] and in vitro [6], the mechanistic details of the mutant's photochemistry were unclear. Recently, we demonstrated that electron transfer on both the reducing- and oxidizing-sides of PS II was seriously compromised in the *psbo1* mutant [10]. Electron transfer from Q_A^- to Q_B in the absence of DCMU, and charge recombination between Q_A^- and the S_2 state of the oxygen-evolving complex in the presence of DCMU, were significantly altered. Additionally, antenna heterogeneity analysis showed the ratio of PS II_α to PS II_β reaction centers was greatly decreased in the *psbo1* mutant due to the absence of the PsbO-1 protein. Finally, flash oxygen yield analysis indicated that both the S_2 and S_3 states exhibited significantly longer lifetimes in the *psbo1* thylakoid preparation than in wild type [10] and that this was the result of the inability of the PsbO-2 protein to efficiently utilize calcium in support of normal oxygen evolution [11]. These data indicated that while PsbO-1-deficient plants can grow photoautotrophically (although at a reduced growth rate) and set seed, the photochemistry of PS II is significantly altered.

In vitro, the importance of the C-terminal domain of the PsbO protein in binding to PS II has been clearly demonstrated [12]. Evaluation of the importance of the N-terminus, however, is more complicated. Seidler reported that an N-terminally His_6-tagged PsbO protein expressed in *Escherichia coli* could reconstitute O_2 evolution to wild-type levels but that its binding characteristics were very different from that of the wild-type protein [13]. It is unclear if the defective binding characteristics observed were due to an alteration of the binding affinity induced by the N-terminal extension or due to inadequate or incorrect refolding of the *E. coli*-expressed protein. Similarly *E. coli*-expressed prePsbO, which contains uncleaved chloroplast and thylakoid membrane transit sequences, was found to fully reconstitute oxygen evolution but was also observed to bind non-specifically to PS II membranes [14]. In this instance, extensive controls were performed to ensure proper refolding of the expressed protein. The domains responsible for the non-specific binding were subsequently identified [15]. Additionally, two domains present at the N-terminus of the protein were identified as being responsible for the binding of the two copies of PsbO observed in higher plants, with only one of these being present in cyanobacterial sequences. It seems likely that the N-terminus of the PsbO protein is exposed, and located near the surface of PSII, rather than being buried either within the tertiary structure of the PsbO protein or at an interface domain of the PsbO protein and the intrinsic components of the photosystem [14].

In our laboratory we are interested in identifying domains of the PsbO protein that are important for PS II function and assembly/stability in vivo. In this communication, a new transformation vector was constructed which contained six histidyl codons located at the N-terminus of the mature PsbO-1 protein coding sequence. The expression of this modified PsbO-1 component was under control of the native *psbO-1* gene promoter. This was introduced into the *A. thaliana psbo1* mutant genome by transformation. Our analysis indicated that the His_6-tagged PsbO-1 protein was expressed and successfully transported into the chloroplast stroma and subsequently into the thylakoid lumen, and was folded into a functionally competent state. The His_6-tagged PsbO-1 protein nearly fully complemented the defective *psbo1* photochemistry that we had previously documented [10].

2. Materials and methods

2.1. Plant materials and growth conditions

Surface-sterilized seeds of wild-type *A. thaliana* (var. *Landsberg erecta*), the mutant *psbo1*, and the transgenic lines were germinated after cold treatment for 24 h at 4 °C on solid MS medium [16] containing 0.7% (w/v) agar. The seedlings were transferred to soil 10 days after germination and grown at 22 ± 0.5 °C under 50–80 μmol photons m^{-2} s^{-1} of white light. Only fully expanded rosette leaves of 4–6 weeks old plants were used for fluorescence analysis. It should be noted that the *psbo1* mutant plants that were used specifically for genetic transformation were grown under different conditions as described below. The *psbo1* mutant was kindly provided by Professor F. Satoh.

2.2. Design and construction of the His_6-psbO-1 gene transformation vector

The pBI121 plasmid was used as the initial shuttle host vector for molecular engineering. Three steps of molecular manipulation were required to obtain the final transformation vector. First, the 35S CMV promoter of pBI121 was replaced with the native *psbO-1* gene promoter. A 680 bp *psbO-1* gene promoter fragment was amplified by PCR using the primers OP68F (all of the PCR primers used in this study are summarized in Table 1) and OP681R using genomic wild-type DNA as a template. This DNA was isolated using DNeasy Plant Mini Kit (Qiagen Sciences, USA). This fragment was then cut with HindIII and XbaI and inserted into pBI121, replacing the original CaMV promoter. In the next step, six-histidine codons were introduced between the DNA sequences that encode the second transit peptide and the mature PsbO-1 sequence. The *psbO-1* gene clone was obtained from The *Arabidopsis* Biological Resource Center (ABRC) and used as the template for PCR. First, a six-histidine codon sequence was added to the 5′ end of the DNA sequence which encodes the mature PsbO-1 protein using the PCR primers HisEGA1 and Msp-1–1133sspI. Second, an AvaI restriction site was included in the primer HisEGA2 that also bears the eighteen base pair sequence encoding the six histidyl residues and was complementary to the bases in the primer HisEGA1. The PCR product generated using the

Table 1
Primers used in this study.

Oligonucleotide	Sequence (length of oligonucleotide)
OP681F	5′-TCTAAGCTTCCCTGCATCCTAGTCCTGAAGT-3′ (31 nt)
OP681R	5′-CAGGTCTAGAAGTCTCTCTTGAGTTTTTTTTTTGGTG-3′ (37 nt)
HisEGA1	5′-CATCACCATCACCATCACGAGGGAGCTCCAAAGAG-3′ (35 nt)
HisEGA2	5′-TCGTCTCGGGAGCAAGTGCGCATCACCATCACCATCAC-3′ (38 nt)
Msp-1–1133ssp-1	5′-CAAAACATGTTAATATTATCATCAAACACAA-3′ (31 nt)
MSP-1-XbaI	5′-AATTCTAGACCATGGCAGCCTCTCTC-3′ (26 nt)
MSP-1–344R-AvaI	5′-ATGCGCACTTGCTCCCGAGACGAC-3′ (24 nt)
psbO-1-SacIF	5′-GGGAGCTCCAAAGAGATTGACC-3′ (22 nt)
psbO-1-SacIR	5′-CTGAGCTCTCACTCAAGTTGACCATACCACACC-3′ (33 nt)
pBINOS7805	5′-ACATGCTTAACGTAATTCAACAG-3′ (23 nt)
Hisprimer	5′-CATCACCATCACCATCAC-3′ (18 nt)
psbO1R813	5′-GGCGTTGTCATATCCTGTG-3′ (19 nt)
PCF	5′-ATGGCCGCAATTACATCAG-3′ (19 nt)
PCR	5′-TTCCCAACCATACCAGCACC-3′ (20 nt)

primers HisEGA2 and primer MSP-1–1133SspI to amplify the DNA template obtained in the first step was cut with AvaI and then ligated with the restricted PCR product using the primer pair MSP-1-XbaI and MSP-1–344R-AvaI. The final XbaI–SspI fragment was inserted into the XbaI and SmaI site of the original vector created in stage one. Finally, in the last step, the PCR product amplified using primers PsbO-1-SacIF and PsbO-1-SacIR was cut with SacI. This fragment was placed in the vector from stage two. The orientation of this insert was confirmed by PCR amplification with the Hisprimer and pBINOS7805 primers. DNA sequencing using the appropriate sequencing primers confirmed the final insert sequence. The final vector was named pHMINTER. All of the molecular manipulations involving *E. coli* followed standard laboratory procedures. The pHMINTER vector was introduced into *Agrobacterium* (strain GV3101) by the freeze–thaw method [17].

2.3. A. thaliana transformation and screening

The stunted size of the *psbo1* mutant plants made transformation difficult. Surface-sterilized *psbo1* seeds were spread onto solid MS medium containing 0.7% agar, 2% sucrose and were incubated in the dark at 4 °C for 2 days. The *psbo1* seedlings were transferred to soil ten days after germination. The plants were grown for two weeks under an 8 h light–16 h dark diurnal cycle at 50–80 μmol photons m^{-2} s^{-1} of white light to encourage vegetative growth. Subsequently, the light cycle was changed manually, increasing the length of the light period and decreasing the length of the dark period by 1 h each day until flowering was induced. The most healthy flowering *psbo1* plants were then transformed with *Agrobacterium* (strain GV3101) containing the pHMINTER plasmid using the floral dip method as described previously [18], except that the Silwet L-77 concentration was decreased to 0.01%. Harvested seeds were surface-sterilized with 50% ethyl alcohol and 0.5% Tween-20 for 3 min and then 70% ethyl alcohol for 3 min followed by washing three times with sterile water. Seeds were spread onto solid MS medium containing 0.7% agar, 50 mg/l kanamycin, and 400 mg/l carbenicillin and then incubated for 2 days at 4 °C in the dark. Transgenic kanamycin-resistant seedlings were transferred to soil when the first true leaves appeared. Four-weeks old fully expanded leaves were used for protein screening analysis and genomic DNA analysis.

The presence of the His_6-tagged PsbO-1-encoding transgene in the genomic DNA of the kanamycin-resistant plant lines was confirmed by PCR using the construct-specific primers Hisprimer and PsbO-1R813. All of the plants that exhibited the kanamycin-resistant phenotype also exhibited the presence of the predicted 470 bp PCR amplification product, which was absent in the wild-type plants and *psbo1* mutant plants (data not shown). Individual kanamycin-resistant plants were screened at the protein level for the presence of the six-histidine region by "Western" blotting. In brief, two leaves from each kanamycin-resistant plant were used for a small-scale thylakoid preparation using the buffers described below. Thylakoid washing was omitted and the thylakoid pellet proteins were tested directly for the presence of His_6-tagged PsbO-1 protein after LiDS-PAGE and "Western" blotting, using an anti-histidine monoclonal antibody (Invitrogen, USA).

2.4. Semi-quantitative RT-PCR analysis

Total RNA was extracted from 100 mg of fresh rosette leaves using RNeasy Plant Mini Kit (Qiagen Sciences, USA) according to the manufacturer's instructions, followed by on-column DNase I treatment to remove any residual genomic DNA contamination. The transcript levels in four-week old plants were examined by semi-quantitative RT-PCR using the transgenic gene-specific primers and the ProtoScript II RT-PCR Kit (NEB, USA) according to the manufacturer's instructions. The primers used were the Hisprimer and PsbO-1R813. The RT-PCR amplification was carried out for 60 min at 42 °C, 4 min at 94 °C, 25 cycles (94 °C for 30 s, 58 °C for 30 s and 72 °C for 45 s), followed by a final extension at 72 °C for 10 min. The RT-PCR reactions were repeated twice, with identical results being obtained. The expression level of plastocyanin was used as an internal control using the primers PCF and PCR.

2.5. Immunological characterization of thylakoid proteins

For a more in-depth analysis of the protein complement of the thylakoid membranes, chloroplast thylakoids were isolated from wild type, the *psbo1* mutant, and two plant lines that expressed different levels of the His_6-tagged PsbO-1 protein. These latter two plant lines were designated *psbo1-C* and *psbo1-M* and expressed high and intermediate amounts of the His_6-tagged PsbO-1 protein, respectively. Leaves were ground in a glass homogenizer with a chloroplast thylakoid isolation buffer (100 mM sucrose, 200 mM NaCl, 5 mM $MgCl_2$, 50 mM sodium potassium phosphate buffer, pH 7.4.), the homogenate was then passed through two layers of Miracloth (Calbiochem USA), and the chloroplast thylakoids were pelleted by centrifugation at 6000 ×*g* for 5 min. The thylakoids were washed once with and resuspended in 300 mM sucrose, 15 mM NaCl, 10 mM $MgCl_2$, and 50 mM MES–NaOH, pH 6.0, and the chlorophyll concentration was determined by the method of Arnon [19]. LiDS-PAGE was performed on a 12.5–20% gradient gel with 5 μg of chlorophyll being loaded per lane. "Western" blotting, blocking, and probing with primary and secondary antibodies were as described previously [5]. For detection of the immobilized antibodies, a chemiluminescent substrate (Super-Signal West Pico Chemiluminescent Substrate, Pierce, USA) was used, and the blots were exposed to X-ray film. After development, the X-ray films were scanned with a UMax PowerLook III scanner at 300-dpi resolution and an 8-bit color depth.

2.6. Fluorescence experiments

Fluorescence induction was monitored with a Photon Systems Instruments (PSI, Czech Republic) FL3000 dual modulation kinetic fluorometer (commercial version of the instrument described in [20]). Both measuring and saturating flashes were provided by computer-controlled photodiode arrays. The flash profile exhibited a square shape for the low power measuring flashes and only deviated 5% from an ideal square shape for the saturating actinic flashes. For all of the fluorescence experiments, single leaves from wild type and the various mutant strains were excised and dark-incubated for 5 min before initiation of the experiments. Data were collected in a logarithmic time series between 10 μs and 1s after the onset of strong actinic light for the PS II closure kinetics analysis [21]. In the flash fluorescence induction experiments, the kinetics of the rapid fluorescence rise following a single saturating flash were examined for 50 μs, with a time resolution of 1 μs in the presence of DCMU. Data were collected at a frequency of 10 MHz with 12 bit resolution. The proportions of PS II_α and PS II_β centers were calculated using proprietary PSI software [20].

In the fluorescence decay experiments, the kinetics of the transfer of an electron between Q_A^- and Q_B were examined in the absence of DCMU, while the recombination reactions of Q_A^- with PS II donor-side components were examined in the presence of DCMU. For these experiments, data were collected between 150 μs and 60 s following a single saturating flash. These were analyzed using the equations outlined in Ref. [22]. In this mathematical treatment, three exponential decay components and a long-lived (essentially non-decaying) residual component were included. In the DCMU treatment experiments, the leaves were immersed in 40 μM DCMU and 0.1% Tween 20 in water and incubated for 30 min prior to performance of the fluorescence experiments. The leaves were dark-adapted for at least 5 min prior to the onset of all fluorescence measurements. Data were

analyzed using Origin version 6.1 and proprietary software provided by Photon Systems Instruments.

3. Results and discussion

3.1. Screening and selection of transgenic plant lines for this study

In this study, we used the native promoter of the *psbO-1* gene to drive the expression of the His_6-tagged *psbO-1* gene instead of using the 35S CaMV promoter that is often used in plant studies. Regulatory element analysis of the *psbO-1* gene promoter [23] indicated that downstream gene expression is light-dependent and organ-specific. The promoter used in this study includes several conserved domains, including the GT1, I, and G boxes, which are light-regulatory elements [23]. Such a combination is hypothesized to integrate light and developmental signals to modulate the promoter activity. The His_6-tagged *psbO-1* gene under the control of its native promoter as used in this study should, in principal, mimic the in vivo expression of the native *psbO-1* gene and minimize any side effects of transgene expression in other tissues. The presence of the His_6-tagged *psbO-1* gene with its native promoter from kanamycin-resistant plants was confirmed by PCR amplification of the *psbO-1* gene promoter region and NOS region from pBI121. All of the plants that exhibited kanamycin resistance also exhibited the expected 1.3 kb PCR amplification product (data not shown). To screen individual transgenic plants for the presence of the six introduced histidyl residues at the N-terminus of the PsbO-1 protein, "Western" blot analysis using an anti-His_6 monoclonal antibody (Invitrogen, USA) and a polyclonal antibody that recognizes both the PsbO-1 and PsbO-2 proteins was performed. Our results indicated that all of the plants that exhibited kanamycin resistance showed the presence of a His_6-tagged protein at about 35 kDa which cross-reacted with the anti-PsbO antibody (data not shown). As expected, individual transgenic plants exhibited different degrees of expression of the His_6-tagged PsbO-1 protein. Several plant lines with variable expression levels of the His_6-tagged PsbO-1 were chosen for the production of homozygous plant lines. After four generations, two homozygous plant lines were selected for use in this study and are designated as *psbo1-M* (about 30% protein expression level of wild type) and *psbo1-C* (about 100% protein expression level of wild type). The growth phenotype of these plants along with wild type and the *psbo1* mutant plant is shown in Fig. 1A. The *psbo1* mutant plants grew quite slowly when compared to wild type and were distinctly paler green in color. The *psbo1-M* plants grew more rapidly than the *psbo1* mutant but not as rapidly as either wild type or the *psbo1-C* plants. The *psbo1-C* plants grew nearly as well as wild type, being only slightly smaller and being slightly less green. Consequently, it appears that the growth phenotype of these plants paralleled the accumulation of the PsbO-1 protein (see below).

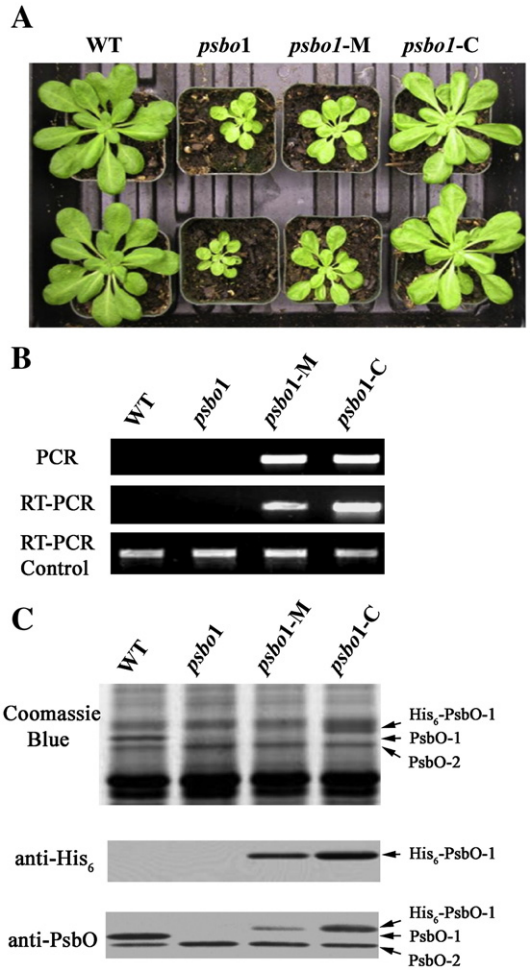

Fig. 1. Molecular and biochemical analysis of transgenic plants. (A) Growth phenotype of wild type, the *psbo1* mutant, and the transgenic plants *psbo1-M* and *psbo1-C*, grown under 50–80 μmol photons m^{-2} s^{-1} of white light. (B) PCR and RT-PCR analysis of genomic DNA and RNA isolated from wild type, the *psbo1* mutant, and the transgenic plants *psbo1-M* and *psbo1-C*. Upper panel, amplification of genomic DNA with primers specific for His_6-tagged PsbO-1-encoding DNA. Middle panel, amplification of reverse transcribed RNA with primers specific for His_6-tagged PsbO-1-encoding DNA. Lower panel, amplification of reverse transcribed RNA with primers specific for plastocyanin-encoding DNA. (C) Analysis of the PsbO proteins present in the thylakoids of wild type, the *psbo1* mutant, and the transgenic plants *psbo1-M* and *psbo1-C*. Upper panel, Coomassie Blue staining of the 28–40 kDa region. Middle panel, immunodetection of His_6-tagged proteins. No other reacting proteins were observed on the "Western blot". Lower panel, immunodetection of the PsbO proteins. The locations of the PsbO-1, PsbO-2 and putative His_6-tagged PsbO-1 proteins are shown to the right. Gel electrophoresis, "Western" blotting and immunodetection were performed as described in Materials and methods. 5 μg of Chl were loaded per lane.

3.2. Increased expression of the His_6-tagged PsbO-1 protein leads to decreased accumulation of the PsbO-2 protein in the thylakoid lumen and increased levels of other PS II components

Fig. 1B illustrates the results of PCR experiments performed on wild type, the *psbo1* mutant and the *psbo1-M* and *psbo1-C* plants using the transgene-specific primers Hisprimer and psbO1R813. In row 1, amplification of genomic DNA isolated from the leaves of the different plant lines indicated that the transgene was present in the *psbo1-M* and *psbo1-C* plants but, as expected, absent in wild type and the *psbo1* mutant plants. In row 2, amplification of reverse transcribed mRNA isolated from the leaves of these plants is shown. Again, no amplification product was obtained from wild type or the *psbo1* mutant plants. An amplification product was observed in both the *psbo1-M* and *psbo1-C* plants, with the apparent transcription level in the *psbo1-C* plant being higher than that observed in the *psbo1-M* plant. This result indicated that the His_6-tagged *psbO-1* transgene was transcribed in the leaves of the *psbo1-M* and *psbo1-C* plants.

Fig. 1C illustrates the accumulation of the different PsbO proteins in the thylakoid membranes of the wild type and mutant plants. In the top panel, Coomassie Blue staining of proteins in the vicinity of the PsbO components is shown. In wild type, both the PsbO-1 and PsbO-2 proteins were observed. As previously reported [9], significantly more PsbO-1 protein was present than PsbO-2 protein. In the *psbo1* mutant no PsbO-1 protein was observed. The PsbO-2 protein was present and accumulated to higher levels than that observed in wild type plants. In both the *psbo1-M* and *psbo1-C* plants, no PsbO-1 protein was observed at its normal location. However a new protein band was observed at about 35 kDa, with more of this component being observed in the *psbo1-C* plant than in the *psbo1-M* plant. This new protein band was identified immunologically in the "Western" blots shown in the lower panels of Fig. 1C. Using the anti-His_6 antibody, no protein band was

observed in either wild type or the *psbo1* mutant. However, in the two transgenic plant lines a protein band was observed at about 35 kDa, at the same position as the new band observed in the Coomassie blue-stained gel. The band present in the *psbo1-C* plant was stronger than that observed in the *psbo1-M* plant. This result indicated that a His_6-tagged protein was present in both of the transgenic plant lines. When probed with the anti-PsbO antibody, the normal pattern of PsbO expression was observed for wild type and the *psbo1* mutant plants. Wild type contained both the PsbO-1 and PsbO-2 proteins, while the *psbo1* mutant contained only the PsbO-2 component. Additionally, more of the PsbO-2 protein was present in the *psbo1* mutant than in wild type. Both transgenic plant lines contained the PsbO-2 protein and lacked the PsbO-1 protein at its normal location. However, at the same location of the His_6-tagged protein, a new protein band appeared which reacted with the anti-PsbO antibody. The band present in the *psbo1-C* plant was stronger than that observed in the *psbo1-M* plant. These data constitute strong evidence that the His_6-tagged PsbO-1 protein encoded by the transgene is expressed, processed and located in the thylakoid membranes of the transgenic plants. It should be noted that the amount of the His_6-tagged PsbO-1 protein appears similar to the amount of untagged PsbO-1 protein present in the wild-type plants.

To determine if the expression of the His_6-tagged PsbO-1 protein leads to alterations in the amounts of other PS II components present in the thylakoids, additional immunological analysis was performed. The relative amounts of some selected PS II components and control proteins were analyzed in thylakoid preparations of wild type, the *psbo1* mutant, *psbo1-M*, and *psbo1-C*, and are shown in Fig. 2. Four proteins that are present in the intrinsic core of PS II (CP47, CP43, D1 and D2) were examined. Qualitative examination of the "Western" blots indicated that the amounts (on a chlorophyll basis) of all of these proteins were somewhat decreased in the *psbo1* mutant when compared to wild type. In the *psbo1-M* and *psbo1-C* plants, the amounts of these proteins increased in parallel with the amount of the His_6-tagged PsbO-1 protein which accumulated. In the *psbo1-C* plant, the amounts of all of these components were near wild-type levels. Loss of the PsbO component has been associated with a decrease in the accumulation of PS II reaction center components in both *Chlamydomonas reinhardtii* [24] and *A. thaliana* [5] mutants. Additionally, our observations confirm and extend earlier results obtained with the

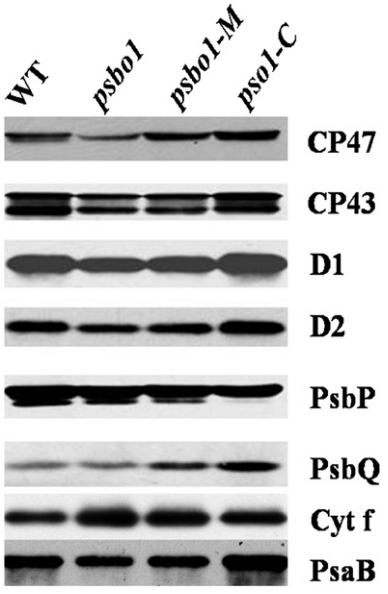

Fig. 2. Immunodetection of the major PS II core components (D1, D2, CP47 and CP43) and other components (Cyt *f* and PsaB) involved in electron transport in chloroplasts. Gel electrophoresis, "Western" blotting and immunodetection were performed as described in Materials and Methods. 5 μg of Chl were loaded per lane.

psbo1 mutant [6]. In addition to the intrinsic PS II core components, the expression of the PsbP and PsbQ extrinsic proteins, which are associated with the oxygen-evolving complex, was also qualitatively examined. In these plants, two immunoreactive bands were observed to be labeled with the anti-PsbP antibody [25]. The PsbP expression pattern of wild type and *psbo1* was generally consistent with that previously reported [9]. Close inspection of the PsbP band in the transgenic plants indicated that slightly less PsbP protein accumulated in the *psbo1-C* plant than the other plants examined. The reason for this is unclear at this time. In reconstitution experiments with PSII membranes preparations, the PsbO protein appeared to be required for the binding of the PsbP protein and the PsbQ proteins [26,27]. It's possible that the exposed N-terminal modification of the PsbO protein may slightly affect a domain that is involved in the binding of the PsbP protein. More interestingly, the PsbQ protein is apparently up-regulated in *psbo1-M* and *psbo1-C* plants, exceeding wild-type (and the *psbo1* mutant) levels. It has been shown that decreased expression of the PsbO proteins in *A. thaliana* led to a dramatic decrease of the PsbQ protein [5]. In *C. reinhardtii*, however, the complete loss of the PsbO protein did not lead to any observable change in the expression of the 17-kDa protein. The elevated level of the PsbQ protein observed here was quite unexpected. It is unclear at this time whether or not the up-regulation of the PsbQ protein in *A. thaliana* was due to the presence of the His_6-tagged PsbO-1 protein. It should be noted that only a proportion of the extrinsic proteins present in thylakoid membranes are functionally associated with the PS II complex; some exist in an unassembled state within a thylakoid lumen pool [28]. Consequently, it is unclear at this time if the apparent increase in the level of the PsbQ component represents protein functionally associated with the photosystem (which we view as unlikely) or the accumulation of free PsbQ protein in the lumenal compartment of the thylakoids.

In addition to these intrinsic and extrinsic components of PS II, we also examined Cyt *f*, a component of the cytochrome b_6/f complex, and PsaB, a reaction center component of PS I. Interestingly, these two proteins appeared to be differentially regulated in the plants we examined. PsaB was down-regulated in the *psbo1* mutant, but appeared in increasing amounts in the two transgenic plant lines, with more protein being detected in *psbo1-C* than in *psbo1-M*. Cyt *f*, however, was up-regulated in the *psbo1* mutant, but appeared in decreasing amounts in the two transgenic plant lines, with less protein being detected in *psbo1-C* than in *psbo1-M*. Earlier, we obtained a similar, although more extreme result, when examining a phenotypic series of plants which expressed variable amounts of the PsbO protein [5]. In that study, decreasing amounts of the PsbO proteins led to a near complete loss of the PsaB component. Re-examination of the immunoblots from that study also indicated that Cyt *f* appeared to increase upon loss of the PsbO proteins and the concomitant loss of assembled PS II. The mechanism(s) leading to the differential expression of these other thylakoid membrane protein complexes upon decreased assembly of PS II are not understood at this time.

3.3. Chlorophyll *a* fluorescence induction

Fig. 3A shows the chlorophyll *a* fluorescence rise during continuous illumination observed in leaves of the wild type, the *psbo1* mutant, *psbo1-M*, and *psbo1-C* plants. Using a logarithmic timing series for the measuring flashes, the polyphasic fluorescence rise exhibited the typical OJIP transients. Qualitatively, the *psbo1* mutant exhibited higher fluorescence yield than wild type over the entire time course of the fluorescence curve. The fluorescence curves of the *psbo1-M* and *psbo1-C* plants lie between those of wild type and the *psbo1* mutant, with the *psbo1-C* plant being very similar to wild type. Quantitative analyses of PS II closure kinetics from the wild type and mutants were evaluated on the basis of a multi-exponential

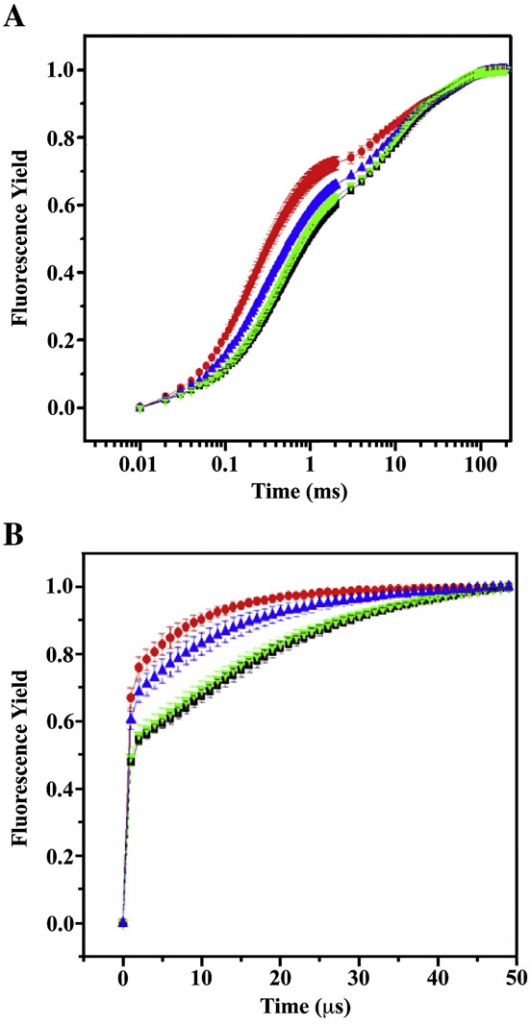

Fig. 3. Chlorophyll fluorescence induction of wild type, the *psbo1* mutant and the transgenic plants *psbo1-M* and *psbo1-C*. A. Fluorescence induction under continuous illumination. B. Fast fluorescence induction in the presence of 40 μM DCMU. In this experiment the fluorescence rise following a single saturating flash was examined at a time resolution of 1 μ s. Please note different time scales in A. and B. Symbols: ■, wild type; ●, *psbo1* mutant; ▲, *psbo1-M*; and, ▼, *psbo1-C*. $n = 3$–5; error bars, ±1.0 s.d.; in some instances the error bars are smaller than the symbols.

analysis of the OJIP fluorescence rise transients [21]. The equations used in this treatment were mathematically derived from the non-linear relationship between fluorescence quantum yield and the fraction of PS II in a closed state [21]. The amplitudes and lifetimes of the OJ, JI, and IP components shown in Table 2 were used to estimate the overall rate constants of the reactions shown in Table 3.

The initial OJ transition constitutes the photochemical phase of the chlorophyll *a* fluorescence rise and can be ascribed to the double reduction of Q_B under conditions when the PQ pool still remains in an oxidized state. PS II closure during this phase is determined by the equilibrium between reduction and reoxidation of Q_B. In our experiment, the k_1 and k_2 rate constants were 1160 s^{-1} and 730 s^{-1}, respectively, while in the *psbo1* mutant k_1 and k_2 were 2470 and 1340 s^{-1}, respectively. The rate constants obtained for wild type are in good agreement with those previously reported in the literature [21,29]. The rate constant k_1 is higher in reaction centers with compromised electron transport between Q_A and Q_B, as this rate constant reflects the rate of Q_A reduction. This was observed in the *psbo1* plant. Its higher k_1 is consistent with our earlier observation of defective electron transport from Q_A^- to Q_B [10] in this mutant. In the *psbo1-M* and *psbo1-C* plants, k_1 and k_2 were observed to decrease to near wild-type values with increasing accumulation of the His_6-tagged PsbO-1 protein. This indicates that the N-terminal His_6-tagged Psbo-1 protein can act as normal PsbO-1 protein in restoring impaired electron transport between Q_A and Q_B in the *psbo1* mutant background.

The JI transition is ascribed to the first phase of PQ pool reduction during which electron transfer from the PQ pool to the Cyt b_6/f complex is maximal [21]. The k_3 and k_4 value can be derived from this transition. In wild type, k_3 and k_4 are 85 s^{-1} and 64 s^{-1}, respectively. The higher k_3 value as compared to k_4 is expected since the value of k_4 in plants growing under optimal conditions is limited by the linear electron flow resulting from PQH_2 oxidation by the Cyt b_6/f complex [30]. Antal and Rubin [21] observed that k_3 and k_4 were 127 s^{-1} and 176 s^{-1}, respectively. The higher k_4 which they observed was unexpected and they speculated that their high k_4 may result either from the changes in fluorescence yield induced by photoelectric trans-thylakoid potential or from the partially reduced state in dark-adapted *C. reinhardtii*. Interestingly, in the *psbo1* mutant, a higher k_4 value (130 s^{-1}) than k_3, (118 s^{-1}) was also observed, which may indicate k_4 is not a limiting factor in the *psbo1* mutant. Our interpretation is that due to the defective oxidizing- and reducing-sides of PS II, the Cyt b_6/f complex is always open for reduction. Alternatively, the Cyt b_6/f complex may be up-regulated, maximizing cyclic electron transport to partially compensate for defective linear electron transport. Our "Western" blot results (Fig. 2) showed that in the *psbo1* mutant, the Cyt *f* subunit was up-regulated compared to wild type, which may provide some evidence to support this hypothesis. In the *psbo1-M* and *psbo1-C* plants, increased levels of the His_6-tagged PsbO-1 protein led to a decrease in the k_3 and k_4 to near wild-type values with increasing accumulation of the His_6-tagged PsbO-1 protein. Finally, the IP phase reflects the further oxidation of the PQ pool due to the establishment of electron flow to electron carriers beyond the Cyt b_6/f complex. The rate constant k_5 is related to overall reduction of intermediates

Table 3
Calculated rate constants for PS II closure.

	k_1, s^{-1}	k_2, s^{-1}	k_3, s^{-1}	k_4, s^{-1}	k_5, s^{-1}	F_V/F_M[a,b]
WT	1160	730	85	64	28	0.79 ± 0.01[b,c]
psbo1	2470	1340	118	130	25	0.58 ± 0.04[c]
psbo1-M	1710	1260	104	95	28	0.75 ± 0.03
psbo1-C	1220	980	82	49	27	0.78 ± 0.01

[a] $n = 3$–5.
[b] Error, ±1.0 standard deviation.
[c] $p < 0.01$ (Student's *t*-test).

Table 2
Quantitative analysis of PS II closure kinetics.

	A_{OJ}	τ_{OJ}, (ms)	A_{JI}	τ_{JI}, (ms)	A_{IP}	τ_{IP}, (ms)
WT	52.7 ± 2.9[a,b,c]	0.45 ± 0.03[c]	27.0 ± 3.0[c]	6.72 ± 1.66	20.3 ± 5.0	35.7 ± 3.0
psbo1	64.9 ± 2.4[c]	0.26 ± 0.01[c]	16.7 ± 2.6[c]	4.03 ± 1.50	18.9 ± 2.9	40.2 ± 7.4
psbo1-M	57.4 ± 0.9	0.34 ± 0.01	22.2 ± 1.0	5.02 ± 0.69	20.6 ± 1.7	35.7 ± 1.5
psbo1-C	55.4 ± 0.5	0.45 ± 0.06	27.8 ± 1.5	7.61 ± 0.19	16.9 ± 0.8	37.3 ± 1.9

[a] $n = 3$–5.
[b] Error, ±1.0 standard deviation.
[c] $p < 0.01$ (Student's *t*-test).

between Cyt b_6/f and FNR. As we see in Table 3, k_5 values from all the plants studied in this chapter were not significantly altered.

Finally, the quantum yield for PS II (F_V/F_M) was evaluated from fluorescence induction data that had not been normalized. As previously reported [9,10], wild-type plants exhibited a high quantum yield (0.79) while the *psbo1* mutant plants exhibited a very low quantum yield (0.58). Both of the transgenic plants, *psbo1-M* and *psbo1-C*, exhibited high quantum yields which were indistinguishable from wild-type values.

3.4. Flash fluorescence induction

Fig. 3B shows the flash-induced fluorescence induction with a 1 μs time resolution in the presence of DCMU. In this experiment, electron transfer between Q_A^- and Q_B is abolished by the presence of the inhibitor. The observed fluorescence rise is the result of the re-reduction by the oxygen-evolving complex of Y_Z, which is in equilibrium with the primary electron donor P_{680}^+ [31]. The shape of this fluorescence rise contains information bearing on the amount of PS II_α and PS II_β reaction centers present in the sample. Exponential fluorescence rise kinetics indicate that the antennae of individual PS II reaction centers are not coupled (i.e., a characteristic of PS II_β centers), while sigmoidal fluorescence rise kinetics indicate a high degree of interconnectivity between the antennae of PS II reaction centers (i.e., a characteristic of PS II_α centers) [32]. This is true under conditions of both continuous relatively weak light illumination (slow fluorescence induction) and single saturating flash conditions (fast fluorescence induction) as demonstrated by Nedbal et al. [20]. In addition to the differences noted above, PS II_β centers have a smaller antenna size, are enriched in chlorophyll *a*, and are depleted of the light-harvesting chlorophyll proteins. They appear to be principally located in the stroma thylakoid membranes [33] and at the granal margins [34]. Additionally, PS II_β centers appear to be defective in their ability to transfer electrons from Q_A^- to Q_B [34].

Qualitative examination of Fig. 3B indicated that, as previously reported [10], wild-type plants exhibited a more sigmoidal fluorescence rise while the *psbo1* mutant exhibited a more exponential fluorescence rise. The two transgenic plants exhibited fluorescence rise kinetics intermediate between these two extremes. The *psbo1-C* plant exhibited a fluorescence rise that was nearly indistinguishable from that of wild type, while the fluorescence rise of the *psbo1-M* plant was more similar to that of the *psbo1* mutant.

Quantitative analysis of these flash fluorescence rise curves allowed the determination of the relative proportions of PS II_α and PS II_β reaction centers present in these plant lines [20]. This analysis is presented in Table 4. In wild type, we found the PS II_α/PS II_β ratio to be 2.59, in line with values obtained in other investigations [10,20,33,35,36]. In the *psbo1* mutant, however, there was a marked enrichment of PS II_β centers, with the PS II_α/PS II_β ratio falling to 0.36, which is consistent with our earlier report [10]. In the *psbo1-C* transgenic plant, the PS II_α/PS II_β ratio was 3.12, within the range observed in the wild-type plant. For unknown reasons we were unable to fit the curve of the *psbo1-M* plant. The increased PS II_α/PS II_β ratio indicated that accumulation of the His_6-tagged PsbO-1 protein led to a decreased amount of PS II_β reaction centers. The high proportion of PS II_β centers which we observed in the *psbo1* mutant may indicate an increased rate of photoinhibition, and thus increased rate of D1 turnover of PS II, since conditions which increase the rate of photoinactivation also lead to increases in the amount of PS II_β centers [35]. This hypothesis was further supported by a recent study using the T-DNA mutants which lack the PsbO-1 and PsbO-2 proteins. In this study, the mutant lacking the PsbO-1 protein was very susceptible to photoinhibition [7].

Table 4
PSII antenna heterogeneity analysis[a].

Strain	$PSII_\alpha$	$PSII_\beta$	$PSII_\alpha/PSII_\beta$
WT	72.2 ± 5.0[b,c]	27.8 ± 5.0[c]	2.59
psbo1	26.7 ± 1.2[c]	73.3 ± 1.2[c]	0.36
psbo1-M	ND	ND	ND
psbo1-C	75.8 ± 6.6	24.2 ± 6.6	3.13

[a] $n = 3–5$.
[b] Error, ± 1.0 standard deviation.
[c] $p < 0.01$ (Student's *t*-test).

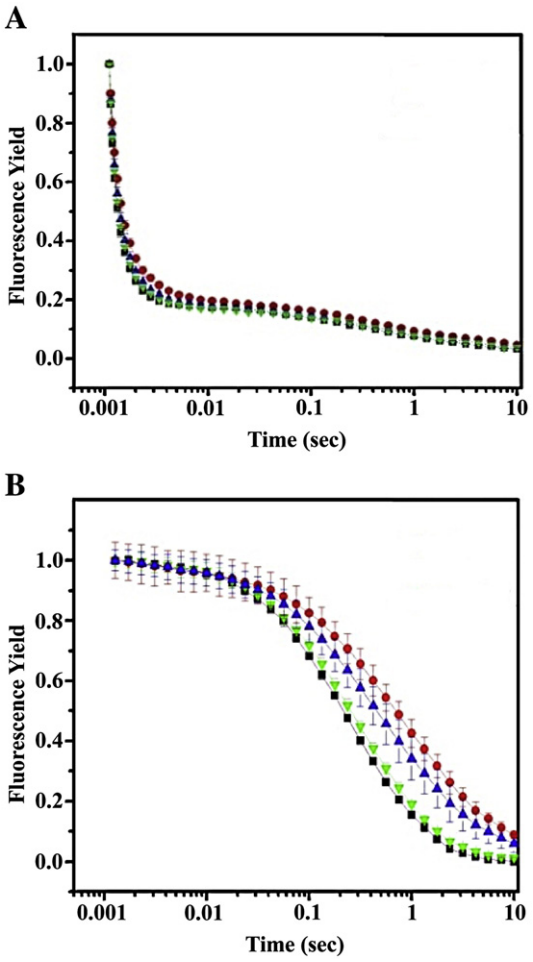

Fig. 4. Chlorophyll fluorescence decay following a single saturating flash in wild type, the *psbo1* mutant and the transgenic plants *psbo1-M* and *psbo1-C*. (A) Fluorescence decay in the absence of DCMU. (B) Fluorescence decay in the presence of 40 μM DCMU. Symbols: ■, wild type; ●, *psbo1* mutant; ▲, *psbo1-M*; and, ▼, *psbo1-C*. $n = 3–5$; error bars, ± 1.0 s.d.; in some instances the error bars are smaller than the symbols.

3.5. Fluorescence decay kinetics

Additional information concerning the electron transfer characteristics on both the reducing- and oxidizing-sides of the photosystem in these plant lines was obtained by examining Q_A^- reoxidation kinetics in either the absence or the presence of DCMU. These results are shown in Figs. 4A and B, respectively. In Fig. 4A the fluorescence decay kinetics of wild type, *psbo1*, *psbo1-M*, and *psbo1-C* in the absence of DCMU are shown. In the absence of DCMU, the fluorescence decay is dominated by electron transfer events that occur on the reducing-side of the photosystem. Qualitatively, the *psbo1* mutant appeared to exhibit somewhat slower fluorescence decay than wild type over the entire time regime examined. The *psbo1-M* and *psbo1-C* transgenic plants exhibited intermediate decay curves, with that of the *psbo1-C* plant's being nearly indistinguishable from wild type. Quantitatively, the fluorescence decay after a single saturating flash can be resolved into three exponential components [22] which are shown in Table 5. It

Table 5
Q_A^- reoxidation kinetics in the absence and presence of DCMU[a].

−DCMU	Fast phase τ (μs)/% amplitude	Middle phase τ (ms)/% amplitude	Slow phase τ (ms)/% amplitude	Residual % amplitude
WT	195 ± 27[b,c]/47.1 ± 4.2	1.02 ± 0.23[c]/29.0 ± 4.3	498 ± 74[c]/17.5 ± 0.6	7.0 ± 0.7
psbo1	324 ± 33[c]/50.8 ± 3.1	2.60 ± 0.78[c]/22.4 ± 2.9	648 ± 51[c]/17.0 ± 0.7	9.3 ± 1.5
Psbo1-M	278 ± 25/53.5 ± 0.7	1.96 ± 0.46/21.7 ± 0.5	595 ± 39/16.7 ± 0.6	7.9 ± 0.7
psbo1-C	213 ± 29/48.5 ± 4.3	1.24 ± 0.28/27.2 ± 4	494 ± 73/17.2 ± 0.5	7.3 ± 0.3
+*DCMU*				
WT	77 ± 11[b,c]/6.1 ± 1.7[c]	274 ± 16[c]/46.3 ± 2.4[c]	1.2 ± 0.1[c]/45.7 ± 1[c]	1.6 ± 1.3[c]
psbo1	4.8 ± 1.5[c]/2.4 ± 1.0[c]	360 ± 20[c]/26.3 ± 3.1[c]	2.5 ± 0.3[c]/59.0 ± 2.5[c]	12.0 ± 1.4[c]
psbo1-M	17.4 ± 7.3[c]/4.1 ± 3.1	342 ± 12[c]/34.2 ± 2.7[c]	2.5 ± 0.1[c]/51.8 ± 2.1	9.2 ± 1.0[c]
psbo1-C	131 ± 21/18.1 ± 3.9[c]	531 ± 75[c]/51.6 ± 3.5	1.9 ± 0.4/28.2 ± 6.0[c]	1.8 ± 0.8

[a] $n = 3$–5.
[b] Error, ± 1.0 standard deviation.
[c] $p < 0.01$ (Student's *t*-test).

should be noted that alternative models containing two exponential decay components and a hyperbolic component [37], or only two exponential decay components, failed to adequately fit the data. The fastest and dominant exponential decay component observed in wild type is related to the transfer of an electron from Q_A^- to Q_B (195 μs, 47.1%). The middle exponential decay component (1.02 ms, 29%) is associated with transfer of an electron from Q_A^- to Q_B in reaction centers which have to bind plastoquinone to the Q_B site before Q_A^- oxidation can occur. The slowest decay component (498 ms, 17.5%) is related to a charge recombination reaction between Q_A^- and donor-side components. Finally, a residual fraction of the fluorescence yield (~7%) is very long-lived and may result from the equilibrium between Q_A^- and Q_B [38]. In the *psbo1* mutant, the time constant for the fast phase modestly increased from 195 to 324 μs. This indicated that electron transport from Q_A^- to Q_B was slowed in the mutant. Additionally, the time constant for the middle exponential decay component increased from 1.02 to 2.6 ms in the mutant. This increase may be related to the large proportion of PS II_β reaction centers present in the mutant. PS II_β reaction centers are localized principally in the stromal thylakoid membranes. Since the stromal membranes are deficient in photochemically reducible plastoquinone [39], the binding of free plastoquinone to the Q_B site would be expected to be slowed in the *psbo1* mutant. The time constant for the slow decay component increased from 498 to 648 ms, indicating a slowing of charge recombination with oxidizing-side components. Finally, the residual amplitude (for the decay component(s) with a $\tau > 10$ s) also increased significantly, perhaps indicating a change in the Q_A^- Q_B equilibrium. Overall, these results indicated that the principal modification on the reducing-side of the photosystem observed in the mutant, the increase in the time constant for the middle exponential decay component, can be explained by the high proportion of PS II_β centers present in the mutant. These results are quite congruent with our earlier findings on wild type and the *psbo1* mutant [10]. In the transgenic plants, the alterations observed in the Q_A^- reoxidation kinetics in the *psbo1* mutant in the absence of DCMU were reversed as the amount of the His_6-tagged PsbO-1 protein increased. All values for the *psbo1-C* plant, which contained wild-type levels of the His_6-tagged PsbO-1 protein, were statistically indistinguishable from wild type. The *psbo1-M* plant, which accumulated an intermediate amount of the His_6-tagged PsbO-1 protein, exhibited decay component values which were between wild type and the *psbo1* mutant values. These results indicate that the His_6-tagged PsbO-1 protein functionally complemented the defects observed on the reducing-side of the *psbo1* mutant.

In the presence of DCMU, which prevents the transfer of an electron from Q_A^- to Q_B, the decay of fluorescence following a saturating flash is dominated by charge recombination between Q_A^- and the oxidizing-side components of the photosystem, principally the S_2 state. Fig. 4B illustrates the fluorescence decay kinetics of wild type, the *psbo1* mutant, and the *psbo1-M* and *psbo1-C* transgenic plants in the presence of DCMU. Qualitatively, the *psbo1* mutant appeared to exhibit slower fluorescence decay than wild type over the entire time regime examined. The *psbo1-M* and *psbo1-C* transgenic plants exhibited intermediate decay curves, with that of the *psbo1-C* plant's being nearly indistinguishable from wild type. The observed fluorescence decay curves were fit to the same model described above [22]. As reported earlier [10], significant alterations were observed in the mutant. In Table 5 the kinetic parameters associated with the observed fluorescence decay in the presence of DCMU are presented. The fastest decaying component observed in wild type exhibited a time constant of 77 μs and is attributed to a small fraction of PS II reaction centers (6.1%) that lack a functional manganese cluster [40] in which Q_A^- recombines directly with oxidized Y_Z. The slowest decay component observed for wild type exhibited a time constant of 1.19 s and is attributed to charge recombination between Q_A^- and the S_2, and possibly the S_3, states [41]. The origin of the intermediate decay component observed in wild type (274 ms) is unclear. In the *psbo1* mutant the fastest decaying component exhibited a time constant of 4.8 μs. The origin of this extremely rapid decaying component is unclear at this time. The slowest decay component was observed to have a time constant of 2.47 s, and its amplitude increased from 45.7% in wild type to 59%. This result indicated that the S_2 state, and possibly the S_3 state, were more stable in the *psbo1* mutant than in wild type. This is supported by our earlier flash oxygen yield analysis [10,11]. Little change was observed for the time constant of the intermediate decay component, although its amplitude decreased from 46.3% in wild type to 26.3% in the mutant. The residual decay component ($\tau > 10$ s) increased nearly 8-fold in amplitude. These results are also quite similar to our earlier findings on wild type and the *psbo1* mutant [10].

In the transgenic plants, most of the alterations observed in the Q_A^- reoxidation kinetics in the *psbo1* mutant in the presence of DCMU were reversed as the amount of the His_6-tagged PsbO-1 protein increased. The time constants of the fast and slow components of the decay in the *psbo1-C* plants were not significantly different from wild-type values. The time constant of the intermediate component was higher in the *psbo1-C* plant than in wild type. As noted above, however, the origin of this decay component is unclear. Consequently, it is difficult to evaluate this difference with respect to the phenotype of the *psbo1-C* plant. Some differences also were apparent in the amplitudes of the different kinetic phases. The fast kinetic phase accounted for a higher proportion of the overall fluorescence decay in the *psbo1-C* plant than in wild type. Conversely, the amplitude of the slow kinetic phase accounted for a higher proportion of the overall fluorescence decay in wild type than in the *psbo1-C* plants. Finally, the residual amplitude for decay component(s) with a rate constant(s) greater than 10 s was the same in both wild type and the *psbo1-C* plant. Generally, the *psbo1-M* plant, which accumulated an intermediate amount of PsbO-1, exhibited decay component values that were between wild-type and *psbo1* values. These results indicated that the

His_6-tagged PsbO-1 protein functionally complemented the majority of the defects observed on the oxidizing-side of the *psbo1* mutant.

4. Conclusions

The *psbo1* mutant exhibits significant defects in PS II photochemistry. In this communication we provide evidence that an N-terminally His_6-tagged PsbO-1 protein can complement the majority of these defects observed on both the reducing- and oxidizing-sides of PS II in the *psbo1* mutant. This is the first report demonstrating that a modified protein can functionally bind to PS II in higher plants in vivo. As noted in the introduction, alterations of the N-terminus of the PsbO protein can have significant consequences in vitro. While PsbO protein mutants containing N-terminal extensions can reconstitute steady state oxygen evolution rates, they typically exhibit significantly altered binding curves [14,42] and require high, non-stoichiometric amounts of protein to achieve full reconstitution of the oxygen evolution activity. In the current study we demonstrate that, at least with respect to an N-terminal His_6-tag, nearly full complementation of the defects observed in the *psbo1* mutant can be achieved even in the absence of abnormally high levels of expression of the transgenic protein. Indeed, our PS II closure kinetics, quantum yield, and Q_A^- reoxidation kinetics (in the absence of DCMU) measurements all indicate that values indistinguishable from wild type are achieved even in the *psbo1-M* plants, which contain relatively low amounts of the His_6-tagged PsbO-1 protein.

In this communication, we have attributed the observed complementation of the *psbo1* mutant phenotype solely to restoration of normal amounts of the PsbO-1 protein. We believe this to be the case. It should be pointed out, however, that it is formally possible that complementation of the mutant phenotype is due to both restoration of normal amounts of the PsbO-1 protein *coupled* with a decrease in the amount of the PsbO-2 component. These two hypotheses cannot be differentiated at this time and will require further study.

We believe that this system will provide a platform for examining the in vivo consequences of other directed mutations in the PsbO-1 protein with respect to photosystem function and assembly. Finally, the engineered transformation vector pHMINTER can be generally used for introducing an N-terminal His_6-tag onto proteins and provides the transit sequences necessary for targeting them to the thylakoid lumen. Since the expression of the engineered protein is driven by the native PsbO promoter, expression levels and subcellular location of the target protein should more closely correspond to the native expression patterns of lumenal proteins.

Acknowledgements

Support for this research was provided by grants from the National Science Foundation and the Department of Energy to T.M.B. and L.K.F.

References

[1] T.M. Bricker, D.F. Ghanotakis, Introduction to oxygen evolution and the oxygen-evolving complex, in: D.R. Ort, C.F. Yocum (Eds.), Oxygenic Photosynthesis: The Light Reactions, Kluwer Academic Publishers, Dordrecht, 1996, pp. 113–136.
[2] T.M. Bricker, R.L. Burnap, The extrinsic proteins of photosystem II, in: T. Wydrzynski, K. Satoh (Eds.), Photosystem II: The Water/Plastoquinone Oxido-Reductase of Photosynthesis, Springer, Dordrecht, 2005, pp. 95–120.
[3] J. Roose, K.M. Wegener, H. Pakrasi, The extrinsic proteins of photosystem II, Photosyn. Res. 92 (2007) 369–387.
[4] T.M. Bricker, Oxygen evolution in the absence of the 33 kDa manganese-stabilizing protein, Biochemistry 31 (1992) 4623–4628.
[5] X. Yi, M. McChargue, S.M. Laborde, L.K. Frankel, T.M. Bricker, The manganese-stabilizing protein is required for photosystem II assembly/stability and photoautotrophy in higher plants, J. Biol. Chem. 280 (2005) 16170–16174.
[6] R. Murakami, K. Ifuku, A. Takabayashi, T. Shikanai, T. Endo, F. Sato, Functional dissection of two *Arabidopsis* PsbO proteins PsbO1 and PsbO2, FEBS J. 272 (2005) 2165–2175.
[7] B. Lundin, M. Hansson, B. Schoefs, A.V. Vener, C. Spetea, The *Arabidopsis* PsbO2 protein regulates dephosphorylation and turnover of the photosystem II reaction center D1 protein. Plant. J. 49 (2007) 528–539.
[8] E. Goulas, M. Schubert, T. Kieselbach, L.A. Kleczkowski, P. Gardestrom, W.P. Schroder, V. Hurry, The chloroplast lumen and stromal proteomes of *Arabidopsis thaliana* show differential sensitivity to short- and long-term exposure to low temperature, Plant. J. 47 (2006) 720–734.
[9] R. Murakami, K. Ifuku, A. Takabayashi, T. Shikanai, T. Endo, F. Sato, Characterization of an *Arabidopsis thaliana* mutant with impared *psb*O, one of two genes encoding extrinsic 33-kDa proteins in photosystem II, FEBS Lett. 523 (2002) 138–142.
[10] H. Liu, L.K. Frankel, T.M. Bricker, Functional analysis of photosystem II in a PsbO-1 deficient mutant in *Arabidopsis thaliana*, Biochemistry 46 (2007) 7607–7613.
[11] T.M. Bricker, L.K. Frankel, The *Arabidopsis psbo1* mutant is cannot efficiently utilize calcium in support of photosynthetic oxygen evolution, J. Biol. Chem. 283 (2008) 29022–29027.
[12] S.D. Betts, N. Lydakis-Simantiris, J.R. Ross, C.F. Yocum, The carboxyl-terminal tripeptide of the manganese-stabilizing protein is required for quantitative assembly into photosystem II and for high rates of oxygen evolution activity, Biochemistry 37 (1998) 14230–14236.
[13] A. Seidler, Introduction of a histidine tail at the N-terminus of a secretory protein expressed in *E. coli*, Protein Eng. 7 (1994) 1277–1280.
[14] H. Popelkova, M.M. Im, J. D'Auria, S.D. Betts, N. Lydakis-Simantiris, C.F. Yocum, N-terminus of the Photosystem II manganese-stabilizing protein: effects of sequence elongation and truncation, Biochemistry 41 (2002) 2702–2711.
[15] H. Popelkova, M.M. Im, C.F. Yocum, Binding of manganese-stabilizing protein to photosystem II: Identification of essential N-terminal threonine residues and domains that prevent nonspecific binding, Biochemistry 42 (2003) 6193–6200.
[16] T. Murashige, F. Skoog, A revised medium for rapid growth and bioassays with tobacco cultures, Physiol. Plant. 15 (1962) 473–479.
[17] M. Holsters, D. de Waele, E. Messens, M. Van Montagu, J. Schell, Transfection and transformation of *Agrobacterium tumefaciens*, Mol. Gen. Genet. 163 (1978) 181–187.
[18] S.J. Clough, A. Bent, Floral dip: a simplified method for *Agrobacterium*-mediated transformation of *Arabidopsis thaliana*, Plant J. 16 (1998) 735–743.
[19] D.I. Arnon, Copper enzymes in isolated chloroplasts. Polyphenol oxidase in *Beta vulgaris*, Plant Physiol. 24 (1949) 1–15.
[20] L. Nedbal, M. Trtílek, D. Kaftan, Flash fluorescence induction: a novel method to study regulation of photosystem II, J. Photochem. Photobiol. B 48 (1999).
[21] T. Antal, A. Rubin, In vivo analysis of chlorophyll a fluorescence induction, Photosyn. Res. 96 (2008) 217–226.
[22] F. Reifarth, G. Christen, A.G. Seeliger, P. Dormann, C. Benning, G. Renger, Modification of the water oxidizing complex in leaves of the *dgd1* mutant of *Arabidopsis thaliana* deficient in the galactolipid digalactosyldiacylglycerol, Biochemistry 36 (1997) 11769–11776.
[23] U. Dasgupta, M. Jain, A.K. Tyagi, J.P. Khurana, Regulatory elements for light-dependent and organ-specific expression of *Arabidopsis thaliana* PSBO1 gene encoding 33 kDa polypeptide of the oxygen-evolving complex, Plant Sci. 168 (2005) 1633–1642.
[24] J.M. Erickson, M. Rahire, P. Malnoe, B.J. Girard, Y. Pierre, P. Bennoun, J.D. Rochaix, Expression of the nuclear encoded OEE-1 protein is required for oxygen evolution and stability of photosystem II particles in *Chlamydomonas reinhardtii*, EMBO J. 6 (1987) 313–318.
[25] X. Yi, H. Liu, S. Hargett, L.K. Frankel, T.M. Bricker, The PsbP protein is required for photosystem II complex assembly/stability and photoautotrophy in *Arabidopsis thaliana*, J. Biol. Chem. 34 (2007) 24833–24841.
[26] B. Andersson, C. Larsson, C. Jansson, U. Ljungberg, H.E. Akerlund, Immunological studies on the organization of proteins in photosynthetic oxygen evolution, Biochim. Biophys. Acta 766 (1984) 21–26.
[27] K. Kavelaki, D.F. Ghanotakis, Effects of the manganese complex on the binding of the extrinsic proteins (17, 23 and 33 kDa) of photosystem II, Photosynth. Res. 29 (1991) 149–155.
[28] W.F. Ettinger, S.M. Theg, Physiologically active chloroplasts contain pools of unassembled extrinsic proteins of the photosynthetic oxygen-evolving enzyme complex in the thylakoid lumen, J. Cell. Biol. 115 (1991) 321–328.
[29] D. Lazar, The polyphasic chlorophyll a fluorescence rise measured under high intensity exciting light, Funct. Plant Biol. 33 (2006) 9–30.
[30] W. Haehnel, Photosynthetic electron transport in higher plants, Ann. Rev. Plant Physiol. 35 (1984) 659–693.
[31] H. Robinson, A. Crofts, Kinetics of the changes in oxidation-reduction states of the aceptors and donors of Photosystem II in pea thylakoids measured by flash fluorescence, in: J. Biggins (Ed.), Martinus Nijhoff/Dr. W. Junk, Den Haag, 1987, pp. 429–432.
[32] J. Lavergne, H.W. Trissl, Theory of fluorescence induction in photosystem II: derivation of analytical expressions in a model including exciton–radical-pair equilibrium and restricted energy transfer between photosynthetic units, Biophys. J. 68 (1995) 2474–2492.
[33] J. Lavergne, J.M. Briantais, Photosystem II heterogeneity, in: D. Ort, C.F. Yocum (Eds.), Oxygenic Photosynthesis: The Light Reactions, Kluwer Academic Publishers, Dordrecht, 1996, pp. 265–287.
[34] L. Wollenberger, H. Stefansson, S.G. Yu, P. Albertsson, Isolation and characterization of vesicles originating from the chloroplast grana margins, Biochim. Biophys. Acta 1184 (1994) 93–102.
[35] A. Melis, Dynamics of photosynthetic membrane composition and function, Biochim. Biophys. Acta 1058 (1991) 87–106.
[36] A. Melis, P.H. Homann, Heterogeneity of the photochemical centers in system II of chloroplasts, Photochem. Photobiol. 23 (1976) 343–350.
[37] Y. Allahverdiyeva, Z. Deak, A. Szilard, B.A. Diner, P.J. Nixon, I. Vass, The function of D1-H322 in photosystem II electron transport studied by thermoluminescence

and chlorophyll fluorescence in site-directed mutants of *Synechocystis* 6803, Eur. J. Biochem. 271 (2004) 3523–3532.
[38] H.H. Robinson, A.R. Crofts, Kinetics of the oxidation reduction reactions of the photosystem II quinone acceptor complex and the pathway for deactivation, FEBS Lett. 153 (1983) 221–226.
[39] A. Melis, J.S. Brown, Stoichiometry of system I and system II reaction centers and of plastoquinone in different photosynthetic membranes, Proc. Natl. Sci. Acad. U. S. A. 77 (1980) 4712–4716.
[40] W. Weiss, G. Renger, Analysis of the system II reaction by UV-absorption changes in Tris-washed chloroplasts, in: C. Sybesma (Ed.), Advances in Photosynthesis Research, Martinus Nijhoff/Dr. W. Junk, Den Haag, 1984, pp. 167–170.
[41] R.J. Debus, The manganese and calcium ions of photosynthetic oxygen evolution. Biochim. Biophys. Acta 1102 (1992) 269–352.
[42] A. Seidler, Expression of the 23 kDa protein from the oxygen-evolving complex of higher plants in *Escherichia coli*, Biochim. Biophys. Acta 1187 (1994) 73–79.